Synthesis, structure, and magnetic studies on self-assembled $BiFeO_3-CoFe_2O_4$ nanocomposite thin films

R. Muralidharan,[1,a)] N. Dix,[1] V. Skumryev,[2] M. Varela,[3] F. Sánchez,[1] and J. Fontcuberta[1]
[1]*Institut de Ciència de Materials de Barcelona-CSIC, Campus UAB, Bellaterra 08193, Spain*
[2]*Institut Català de Recerca i Estudis Avançats (ICREA), Barcelona, Spain*
[3]*Departament de Física Aplicada i Òptica and Institut de Nanociència i Nanotecnologia (IN2UB), Universitat de Barcelona, Diagonal 647, Barcelona 08028, Spain*

(Presented on 9 November 2007; received 12 September 2007; accepted 17 December 2007; published online 5 February 2008)

Self-assembled $(0.65)BiFeO_3-(0.35)CoFe_2O_4$ (BFO-CFO) nanostructures were deposited on $SrTiO_3$ (001) and (111) substrates by pulsed laser deposition at various temperatures from 500 to 800 °C. The crystal phases and the lattice strain for the two different substrate orientations have been determined and compared. The films grow epitaxial on both substrates but separation of the spinel and perovskite crystallites, without parasitic phases, is only obtained for growth temperatures of around 600–650 °C. The BFO crystallites are out-of-plane expanded on STO(001), whereas they are almost relaxed on (111). In contrast, CFO crystallites grow out-of-plane compressed on both substrates. The asymmetric behavior of the cell parameters of CFO and BFO is discussed on the basis of the role of the epitaxial stress caused by the substrate and the spinel-perovskite interfacial stress. It is concluded that interfacial stress dominates the elastic properties of CFO crystallites and thus it may play a fundamental on the interface magnetoelectric coupling in these nanocomposites. © *2008 American Institute of Physics*.
[DOI: 10.1063/1.2832346]

I. INTRODUCTION

Multiferroic materials are attractive because they have two ferroic properties and the interactions between the magnetic and electric polarizations lead to additional functionalities. However, having multiferroic materials with ferroelectricity and ferromagnetism in a single phase is difficult.[1,2] The single phase magnetoelectric materials reported so far have either too weak coupling at room temperature or coupling occurs at very low temperature.[3–5] A self-assembled nanostructure with ferro(ferri)magnetic nanopillars embedded in a ferroelectric matrix or vice versa and their magnetoelectric coupling by lattice strain mediation is an appealing alternative. Zheng *et al.* reported a model system of $BaTiO_3-CoFe_2O_4$ nanostructures which was multiferroic and showed magnetoelectric coupling.[6] Several other combinations with immiscible perovskites ($BiFeO_3$, $PbTiO_3$) and spinels ($NiFe_2O_4$, $CoFe_2O_4$) prepared by pulsed laser deposition self-assemble into nanostructures too.[7–9] Recently, it has been reported that by using sputtering as deposition technique, in which the growth rate is lower, phase separation can occur at lower temperature.[10] Remarkably, Zavaliche *et al.*[7] demonstrated the electric field induced magnetization reversal at room temperature for $BiFeO_3-CoFe_2O_4$ (BFO-CFO) nanostructures, creating high interest in this system.

It has been reported that elastic coupling between the perovskite and spinel system plays a major role in determining both the epitaxy and the magnetoelectric coupling of these nanocomposites.[11,12] Therefore, the study of the lattice strain becomes very important to understand the strain mediation in these nanostructures. However surprisingly not much has been reported on the dependence of lattice strain of the perovskite and spinel system with growth temperature and on different substrate orientations.

In this paper, we report our experimental results on the growth of BFO-CFO nanostructures on $SrTiO_3$ (STO) substrates with different orientations, (001) and (111). The influence of growth temperature on the crystal phases and their strain is investigated. Phase separation and magnetic characterization at the nanoscale is also studied by means of magnetic force microscopy.

II. EXPERIMENTAL

The BFO-CFO nanocomposite thin films were prepared on STO (001) and (111) substrates by pulsed laser (KrF excimer) deposition with a repetition rate of 5 Hz. The target, with 10% excess of bismuth, was prepared by conventional solid state reaction. The substrate temperature was varied from 500 to 800 °C and substrates with different orientations were placed simultaneously to ensure the same growth conditions. The oxygen pressure was maintained at 0.1 mbar. The films have similar thickness of about 100 nm.

The crystal structure of films was analyzed using x-ray diffraction (XRD) by Cu Kα θ-2θ scans of symmetrical reflections and φ scans of asymmetrical reflections. Field emission scanning electron microscopy (FESEM) was used to investigate the surface morphology. Magnetic force microscopy (MFM) with Si tip coated with Co–Cr in the tapping lift mode was utilized to view the local magnetic domains.

III. RESULTS AND DISCUSSION

Figures 1(a) and 1(b) show XRD θ-2θ scans of the (001) and (111) samples, respectively. The temperature indicated in

a)Electronic mail: mrajaram@icmab.es.

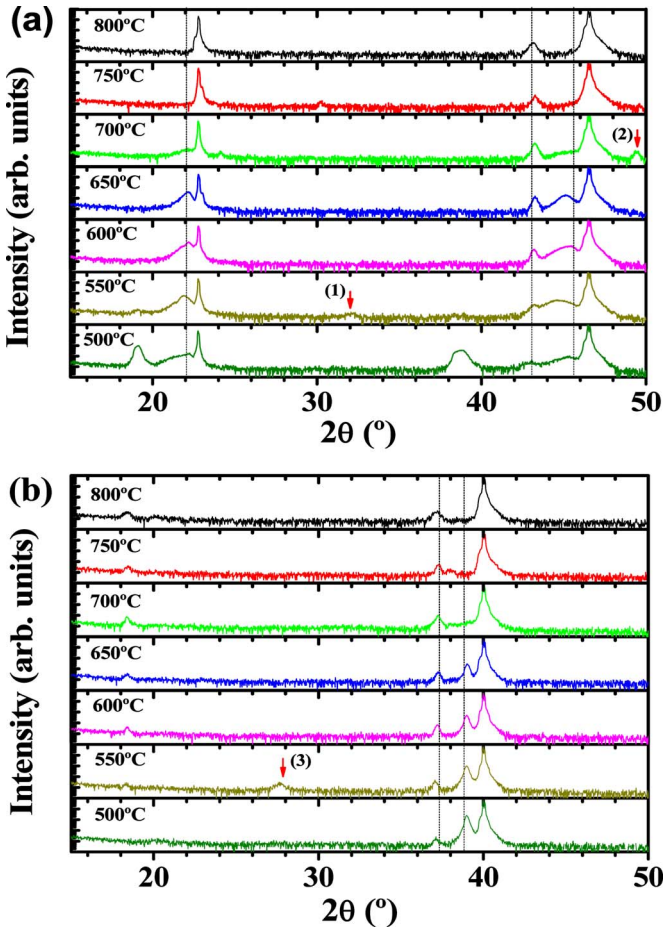

FIG. 1. (Color online) XRD θ-2θ pattern for the BFO-CFO nanostructures grown on (a) STO(001) substrates (b) STO(111) substrates at various temperatures. Diffracted intensity is plotted in logarithmic scale. Diffraction peaks from parasitic phases are marked: (1) Bi_2O_3(321), (2) Fe_2O_3(024), and (3) Bi_2O_3(310).

each θ-2θ scan corresponds to the film growth temperature (T_S). We first consider the effects of varying T_S on the structure of films grown on STO (001) [Fig. 1(a)]. The most intense peaks around 2θ=22.7° and 46.4° correspond to the (001) and (002) substrate reflections, respectively. The others are diffraction peaks from the films. In the case of films deposited at 600 or 650 °C only the (001) and (002) reflections of BFO and the (004) reflection of CFO are observed. Vertical dotted lines in Fig. 1(a) indicate the positions of these reflections as inferred from corresponding bulk cell parameters [$a(BiFeO_3)$=0.396 nm and $a(CoFe_2O_4)$=0.839 nm (Refs. 13 and 14)]. Thus, the films grown on STO (001) at T_S=600–650 °C display the coexistence of the perovskite phase and spinel phases with out-of-plane cell parameters close to bulk ones; a clear (00l) texture is observed. On the other hand, XRD φ scans for the samples deposited at 650 °C (not presented here) showed that the two phases grow epitaxially with [100]BFO(001)‖[100]STO(001) and [100]CFO(001)‖[100]STO(001) epitaxial relationships. Importantly, no other reflections are observed in the films grown at T_S=600–650 °C (notice that the intensity is plotted in logarithmic scale in Fig. 1). On the other hand, in the XRD of films grown at lower temperature (T_S=550 °C), although they still show the presence of distinguishable and

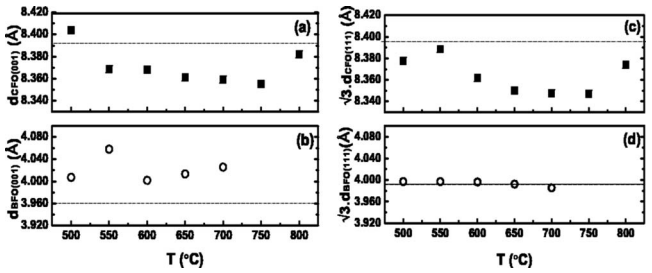

FIG. 2. Temperature dependence of out-of-plane lattice parameter for (a) CFO(001), (b) BFO(001), (c) CFO(111), and (d) BFO(111). Dashed lines indicate the bulk values.

c-axis textured CFO and BFO phases, one can also appreciate the existence of a very small reflection at $2\theta \approx 32°$, that can be assigned to Bi_2O_3(321). XRD patterns of films grown at even lower temperature display the progressive appearance, well visible at T_S=500 °C of two broad peaks centered at around $2\theta \approx 19°$ and 38°. Their positions between those expected for (111) textured crystallites of CFO and BFO suggests the formation of a solid solution. Films grown at much higher temperatures (T_S=700, 750, and 800 °C) show a progressive reduction, even suppression, of the intensity of the BFO reflections and only the spinel CFO (004) peak remains well visible. It should be also noticed that at about $2\theta \approx 49.3°$, an incipient reflection indexable as Fe_2O_3(024) develops. Disappearance of BFO signatures and the accompanying presence of Fe_2O_3 traces in the XRD pattern would both result from bismuth evaporation at high temperature. In earlier works on single phase $BiFeO_3$ thin films,[15,16] parasitic Bi_2O_3 and Fe_2O_3 were also reported to appear at low and high growth temperatures, respectively.

We consider now the films on STO(111) substrates. The most intense peaks at $2\theta \approx 40°$ in Fig. 1(b) correspond to the (111) substrate reflection. The peaks around $2\theta \approx 37°$ and 39° correspond to the CFO(222) and BFO(111) reflections, respectively, thus indicating that CFO and BFO grow (111) textured. Similarly to what was found for films on (001) substrates, the XRD patterns of films grown at T_S =600–650 °C reveal the presence of fully (111) textured BFO and CFO phases without any parasitic phase. On the other hand, XRD φ scans for the samples grown at 650 °C (not presented here) showed that the two phases grow epitaxially with [1−10]BFO(111)‖[1−10]STO(111) and [01−1]CFO(111)‖[1−10]STO(111) epitaxial relationships. Interestingly enough, and in contrast to what was observed on STO(001) substrates, coexisting BFO and CFO phases are still well visible in films grown at lower temperature (down to T_S=500 °C) although the presence of segregated Bi_2O_3 is revealed by the Bi_2O_3(310) reflection well visible in the T_S =550 °C pattern at 2θ=27.6°. Films grown at higher (T_S >650 °C) also follow the same trend as in the case of (001) substrate, with only CFO reflections visible likely due to bismuth volatility. Therefore, the growth temperature window for impurity-phase free (at XRD sensitivity level) BFO-CFO nanocomposite growth (001) and (111) STO substrates is thus found to be similar.

The out-of-plane lattice parameters of CFO and BFO are depicted against the substrate temperature in Figs. 2(a)–2(d).

Figures 2(b) and 2(d) reveal that the BFO(001) crystallites are highly strained, with an out-of-plane strain of ~1%, the BFO(111) crystals are almost relaxed (the strain is lower than ~0.1%). The BFO out-of-plane strain corresponds to an expansion, as expected as there is an in-plane compressive epitaxial stress [bulk BFO lattice parameter is longer (0.396 nm) than that of STO (0.3905 nm)]. Therefore, although the lattice mismatch parameter between the STO substrate and the BFO structure in the (001) and (111) textures is identical, the subsequent elastic deformation of BFO is radically different.

On the other hand, CFO crystallites appear to be similarly strained on both substrates; the out-of-plane parameter of CFO is found to be somewhat smaller than that of bulk CFO: around −0.4% and −0.6% for (001) and (111) crystals, respectively. However, the strain corresponds to a compression; we emphasize that according to the bulk cell parameters of CFO and STO and assuming the most common scenario of elastic epitaxy-induced deformation of lattices, in-plane epitaxial compression, and subsequent out-of-plane expansion should be expected. A similar effect on another nanocomposite ($BaTiO_3$–$CoFe_2O_4$) was reported recently and it was suggested that the unexpected CFO lattice strain could be due to the stress caused by the ferroelectric $BaTiO_3$ matrix rather than the substrate.[10,17] Therefore, we should conclude that stress caused by the substrate is not the driving force for the observed strain in CFO but the interface BFO/CFO should play a major role and considering the dissimilar strains observed in the BFO grown on STO(001) and (111) substrates, the corresponding interfaces should be markedly different.

It is clear from the FESEM images, in agreement with earlier reports,[18] that the microstructure of BFO/CFO nanocomposites on (001) and (111) STO substrates drastically differ: whereas nanopillars of CFO in a BFO matrix are formed on (001) STO, nanopillars of BFO in a CFO matrix are obtained on (111)STO and subsequently, different interfaces are formed. In Figs. 3(a) and 3(b), the FESEM images of the films grown at 650 °C on (001) and STO (111) are shown.

The ferromagnetic character of the nanopillars formed on (001) has been monitored by comparing the topographic and magnetic force images [Figs. 3(c) and 3(d), respectively] collected with the MFM microscope on the film deposited on STO(001) at 650 °C. The topographic image confirms the expected very rough surface, with height variations up to 80 nm. First the as-grown sample without any magnetic treatment was viewed to know the initial magnetic state and dark and bright structures were clearly observed (not shown here) indicating that the sample has both up and down magnetic domains coinciding with the pillars observed in the topographic image. Later, the sample was measured after magnetizing it under 1 T. The phase image, shown in Fig. 3(d), clearly shows that most of the domains are oriented in one direction; they appear black implying repulsive forces between the tip and the nanodomains. This was confirmed by reversing the magnetization of the tip and subsequent contrast switching.

In summary CFO-BFO nanostructures on STO(001) and (111) substrates were prepared at various temperatures. It was found that the window to obtain CFO-BFO phase separation without any parasitic phase is quite narrow (600–650 °C) and similar for both substrates. The analysis of the lattice strain on the resulting CFO-BFO nanocomposites allows us to conclude that CFO-BFO interface strain appears to overcome the epitaxial stress caused by the substrate and dominates the elastic response of CFO crystallites. This observation may have impact on understanding the microscopic nature of the reported magnetoelectric coupling in similar nanocomposites.

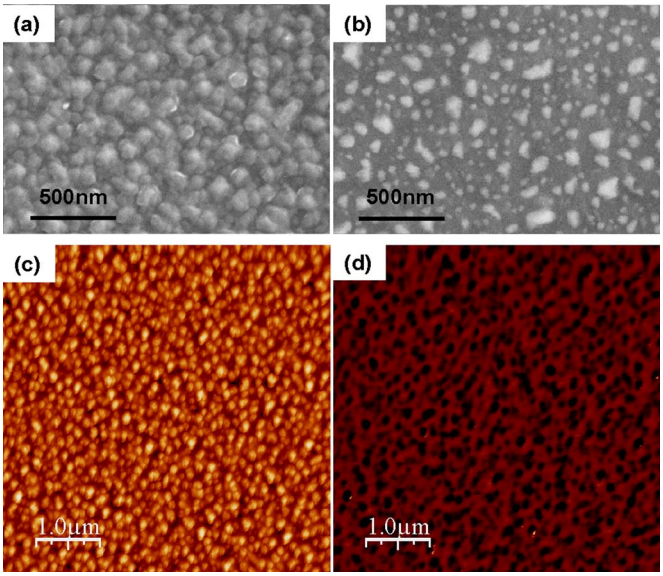

FIG. 3. (Color online) [(a) and (b)] FESEM images for films grown at 650 °C on STO(001) and (111), respectively. [(c) and (d)] MFM topographic and phase images, respectively, from a sample grown on STO(001) at 650 °C. The scan was done after magnetizing the sample with 1 T.

ACKNOWLEDGMENTS

Financial support by the MEC of the Spanish Government (Project Nos. NAN2004-9094-C03, MAT2005-5656-C04, and Nanoselect CSD2007–00041), by CSIC (Project No. 200660I172), and by the European Union (project MaCoMuFi (FP6-03321) and FEDER) is acknowledged.

[1] R. Ramesh and N. A. Spaldin, Nat. Mater. **6**, 21 (2007).
[2] N. A. Spaldin and M. Fiebig, Science **309**, 391 (2005).
[3] N. Hur *et al.*, Nature (London) **429**, 392 (2004).
[4] R. Tackett *et al.*, Phys. Rev. B **76**, 024409 (2007).
[5] Y. Yamasaki *et al.*, Phys. Rev. Lett. **96**, 207204 (2006).
[6] H. Zheng *et al.*, Science **303**, 661 (2004).
[7] F. Zavaliche *et al.*, Nano Lett. **5**, 1793 (2005).
[8] I. Levin *et al.*, Adv. Mater. (Weinheim, Ger.) **18**, 2044 (2006).
[9] Q. Zhan *et al.*, Appl. Phys. Lett. **89**, 172902 (2006).
[10] N. Dix *et al.*, Mater. Sci. Eng., B **144**, 127 (2007).
[11] J. Slutsker *et al.*, Phys. Rev. B **73**, 184127 (2006).
[12] C. W. Nan *et al.*, Phys. Rev. Lett. **94**, 197203 (2005).
[13] Joint Committee on Powder Diffraction Standards, ASTM, Philadelphia, PA, 2000, Card No. 72-2035.
[14] Joint Committee on Powder Diffraction Standards, ASTM, Philadelphia, PA, 2000, Card No. 22-1086.
[15] H. Bea *et al.*, Appl. Phys. Lett. **87**, 072508 (2005).
[16] M. Murakami *et al.*, Appl. Phys. Lett. **88**, 112505 (2006).
[17] H. Zheng *et al.*, Appl. Phys. Lett. **90**, 113113 (2007).
[18] H. Zheng *et al.*, Adv. Mater. (Weinheim, Ger.) **18**, 2747 (2006).